A LETTERS JOURNAL EXPLORING
THE FRONTIERS OF PHYSICS

Phase diagram and superconducting density of states of the quasi-two-dimensional *d*-wave superconductor in parallel magnetic field

To cite this article: Biao Jin 2005 *EPL* **72** 270

EUROPHYSICS LETTERS 15 October 2005

Europhys. Lett., **72** (2), pp. 270–274 (2005)
DOI: 10.1209/epl/i2005-10229-5

Phase diagram and superconducting density of states of the quasi-two-dimensional d-wave superconductor in parallel magnetic field

Biao Jin

College of Physical Science, Graduate School of the Chinese Academy of Sciences P.O. Box 3908, Beijing 100039, PRC

received 21 March 2005; accepted in final form 19 August 2005
published online 14 September 2005

PACS. 74.20.Rp – Pairing symmetries (other than s-wave).
PACS. 74.25.Dw – Superconductivity phase diagrams.
PACS. 74.25.Fy – Transport properties (electric and thermal conductivity, thermoelectric effects, etc.).

Abstract. – We report on results of a theoretical study of the d-wave Fulde-Ferrell-Larkin-Ovchinnikov (FFLO) state. A complete temperature *vs.* magnetic field phase diagram for a model system is obtained. This phase diagram comprises the normal phase, the zero-momentum pairing BCS phase and two types of FFLO phases. The magnetic-field variation of the superconducting density of states, $N_S(\varpi)$, is studied systematically. In the FFLO phase, we find a characteristic multi-peak structure in $N_S(\varpi)$, followed by its unique evolution. These highly distinctive features enable us to discriminate between the d-wave FFLO state and other types of superconducting states.

Introduction. – In 1964, Fulde and Ferrell [1] and Larkin and Ovchinnikov [2] independently predicted that if the superconducting state in uniform high magnetic field is limited by the pair-breaking mechanism alone, the transition from the zero-momentum pairing BCS superconducting state to the normal state may proceed via an interposed inhomogeneous superconducting state (FFLO state). Within the FFLO state, spin-up and spin-down electrons of a spin-singlet superconductor can only stay bound if the Cooper pair has a finite total momentum. Consequently, the FFLO state is formed with a spatially modulating order parameter, and thus is an example of spontaneous spatial symmetry breaking. The FFLO state is also considered to be a candidate for the mechanism of the high-field superconductivity. It is realized that the favourable experimental condition for observing the FFLO state is provided by a very clean superconductor with the Ginzberg-Landau parameter κ much larger than unity. Since these features are not easily satisfied in most conventional superconductors, experimental investigations consider unconventional superconductors such as high-T_c cuprate superconductors, heavy-fermion and organic superconductors, where the above conditions appear to be met [3,4]. These unconventional superconductors are often of quasi-two-dimensional type, so that when a magnetic field is applied parallel to the conducting layers, the orbital pair-breaking effect is minimized and the Zeeman effect dominates the physics, favoring the FFLO state. Theoretically, it is shown that in d-wave superconductors the region of the FFLO phase is much more extended than in s-wave superconductors [5–7]. Indeed, several authors suggested the existence of FFLO states [3], *e.g.*, based on the superconducting phase diagram or the magnetothermal transport properties. However, it seems to be difficult to establish the existence of the FFLO state via these properties alone [8]. More theoretical studies are required to reveal the intrinsic physical properties peculiar to the FFLO state. In this letter, we study the response of the quasi-two-dimensional $d_{x^2-y^2}$ superconducting system to a parallel magnetic field. We first discuss the temperature *vs.* magnetic-field phase diagram of a model system, and then calculate the magnetic-field dependence of $N_S(\varpi)$ over the whole range of temperatures.

Model. – Let us consider a quasi-two-dimensional superconductor with a magnetic field applied parallel to the conducting layers. The system is assumed to be described effectively by the following two-dimensional electron Hamiltonian:

$$H = \sum_{\boldsymbol{k}\sigma} \xi_{\boldsymbol{k}\sigma} c^\dagger_{\boldsymbol{k}\sigma} c_{\boldsymbol{k}\sigma} + \sum_{\boldsymbol{k}\boldsymbol{k}'} V_{\boldsymbol{k}\boldsymbol{k}'} c^\dagger_{\boldsymbol{k}+\boldsymbol{q}/2,\uparrow} c^\dagger_{-\boldsymbol{k}+\boldsymbol{q}/2,\downarrow} c_{-\boldsymbol{k}'+\boldsymbol{q}/2,\downarrow} c_{\boldsymbol{k}'+\boldsymbol{q}/2,\uparrow} \tag{1}$$

with $\xi_{k\sigma} = \xi_{\boldsymbol{k}} - \sigma h$, $\xi_{\boldsymbol{k}} = \epsilon_{\boldsymbol{k}} - \mu$ and $h = \mu_B B$ and where $V_{\boldsymbol{k}\boldsymbol{k}'}$, μ, B and μ_B are, respectively, the pairing interaction between electrons with total momentum $\boldsymbol{q}$, the chemical potential, the magnetic field and the Bohr magneton. We take $V_{\boldsymbol{k}\boldsymbol{k}'} = -V\, g_{\boldsymbol{k}}\, g_{\boldsymbol{k}'}$, and $g_{\boldsymbol{k}} = \cos(2\theta_{\boldsymbol{k}})$ for $d_{x^2-y^2}$ pairing, where $\theta_{\boldsymbol{k}}$ is the azimuthal angle of $\boldsymbol{k}$. For the sake of simplicity, we assume a rotationally invariant band dispersion $\epsilon_{\boldsymbol{k}}$. The standard mean-field treatment followed by the Bogoliubov-Valatin transformation for our Hamiltonian readily yields the quasiparticle Hamiltonian:

$$H_{MF} = \sum_{\boldsymbol{k}\sigma} E^{\boldsymbol{q}}_{\boldsymbol{k}\sigma} \alpha^\dagger_{\boldsymbol{k}\sigma} \alpha_{\boldsymbol{k}\sigma} + \text{const}, \tag{2}$$

with $E^{\boldsymbol{q}}_{\boldsymbol{k}\sigma} = E_{\boldsymbol{k}} + \sigma[q^* \cos(\theta_{\boldsymbol{k}} - \theta_{\boldsymbol{q}}) - h]$, $E_{\boldsymbol{k}} = \sqrt{\xi^2_{\boldsymbol{k}} + \Delta^2_{\boldsymbol{k}}}$, $\Delta_{\boldsymbol{k}} = \Delta g_{\boldsymbol{k}}$ and $q^* = v_F\,|\boldsymbol{q}|\,/2$ and where $\Delta_{\boldsymbol{k}}$, v_F and $\theta_{\boldsymbol{q}}$ are the gap function, the Fermi velocity and the azimuthal angle of the pairing momentum $\boldsymbol{q}$, respectively. The gap parameter Δ is determined by the gap equation

$$1 = VN(0) \int_0^{\varpi_c} \mathrm{d}\xi_{\boldsymbol{k}} \int_0^{2\pi} \frac{\mathrm{d}\theta_{\boldsymbol{k}}}{2\pi} g^2_{\boldsymbol{k}} \left[\tanh\left(\frac{E^{\boldsymbol{q}}_{\boldsymbol{k}\uparrow}}{2T}\right) + \tanh\left(\frac{E^{\boldsymbol{q}}_{\boldsymbol{k}\downarrow}}{2T}\right)\right] / (2E_{\boldsymbol{k}}), \tag{3}$$

where $N(0)$ is the DOS of the normal state at the Fermi energy and ϖ_c the cutoff energy.

Phase diagram. – Here let us examine the (T, H)-phase diagram of the present model. We note that a full account of phase transition requires the knowledge of the free energy, in general, and that the pairing momentum $\boldsymbol{q}$ should be chosen to minimize the free energy for given values of T and H. Here, we calculate the free energy of the superconducting state relative to normal state using the formula

$$F_S - F_N = \int_0^\Delta \mathrm{d}\Delta' \Delta'^2 \mathrm{d}(1/V)/\mathrm{d}\Delta'. \tag{4}$$

We have observed three types of superconducting states: the zero-momentum pairing BCS state and two types of finite-momentum pairing states (henceforth referred to as FFLO-1 state and FFLO-2 state, respectively). In the FFLO-1 state, the pairing momentum $\boldsymbol{q}$ points in the direction of minimum gap ($\theta_{\boldsymbol{q}} = \pi/4$, etc.). In the FFLO-2 state, however, $\boldsymbol{q}$ points in

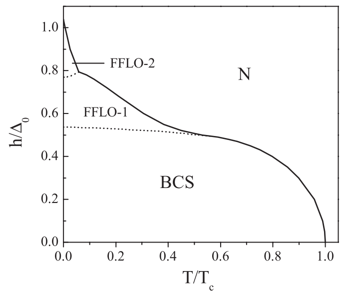

Fig. 1

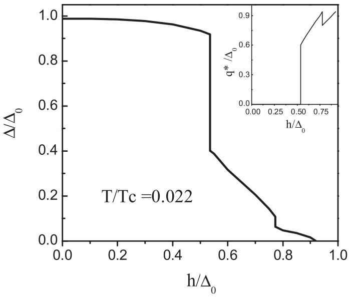

Fig. 2

Fig. 1 – (T, H)-phase diagram of the system described by the Hamiltonian (1). Three types of superconducting phases (BCS, FFLO-1 and FFLO-2) are observed. The lower dotted line is the first-order transition curve between the zero-momentum pairing BCS state and the FFLO-1 state. The upper dotted line denotes the first-order phase boundary separating FFLO-1 and FFLO-2 states. The solid line is the second-order transition curve between the normal state and the superconducting states.

Fig. 2 – The magnetic-field dependence of the gap parameter Δ at $T = 0.022T_c$, where $h_{c1} = 0.54\Delta_0$, $h^*_{c1} = 0.77\Delta_0$ and $h_{c2} = 0.92\Delta_0$. The inset shows the magnetic-field dependence of q^* at the same temperature. Both Δ and q^* undergo discontinuous change at h_{c1} and h^*_{c1}.

the direction of maximum gap ($\theta_{\boldsymbol{q}} = 0$, etc.). The resultant phase diagram is shown in fig. 1. The solid line, in fig. 1, denotes the second-order transition curve between the normal state and the three types of superconducting states, the lower dotted line the first-order transition curve between the zero-momentum pairing BCS state and the FFLO-1 state, and the upper dotted line is the first-order phase boundary separating the FFLO-1 state and the FFLO-2 state. As a consequence, our phase diagram exhibits two tricritical points; one is located at $T = 0.56T_c$, $h = 0.5\Delta_0$, and the other at $T = 0.06T_c$, $h = 0.8\Delta_0$, where T_c is the BCS superconducting transition temperature and Δ_0 the BCS gap parameter at $T = 0$. Figure 2 shows the magnetic-field dependence of the gap parameter Δ at $T = 0.022T_c$. Shown in the inset is the magnetic-field dependence of q^* at the same temperature. As is readily seen, both the gap parameter and q^* change discontinuously across the two first-order phase boundaries. We note that our result on the second-order transition curve between the normal state and the superconducting states agrees with that obtained in the previous studies [5–7]. However, in these works, the upper first-order transition curve was not located and the lower first-order phase boundary was approximated by the one that can be obtained assuming the absence of the FFLO state, which lies slightly above our curve.

Superconducting DOS. – Now, we proceed to investigate the responses of the superconducting DOS, $Ns(\varpi)$, to the magnetic field in different temperature regions. We calculate $Ns(\varpi)$ using the general relation

$$N_S(\varpi) = -\,N(0)\sum_{\sigma}\int_{-\varpi_c}^{\varpi_c}\mathrm{d}\xi_{\boldsymbol{k}}\int_0^{2\pi}\frac{\mathrm{d}\theta_{\boldsymbol{k}}}{2\pi}\,\mathrm{Im}\,G^R_\sigma(\boldsymbol{k},\varpi)/\pi, \tag{5}$$

where $G^R_\sigma(\boldsymbol{k},\varpi)$ is the retarded single-particle Green's function given in the mean-field theory by

$$G^R_\sigma(\boldsymbol{k},\varpi) = u_{\boldsymbol{k}}/(\varpi - E^{\boldsymbol{q}}_{\boldsymbol{k}\sigma} + i0) + v_{\boldsymbol{k}}/(\varpi + E^{\boldsymbol{q}}_{\boldsymbol{k}-\sigma} + i0), \tag{6}$$

with

$$u^2_{\boldsymbol{k}} = (1 + \xi_{\boldsymbol{k}}/E_{\boldsymbol{k}})/2, \qquad v^2_{\boldsymbol{k}} = (1 - \xi_{\boldsymbol{k}}/E_{\boldsymbol{k}})/2. \tag{7}$$

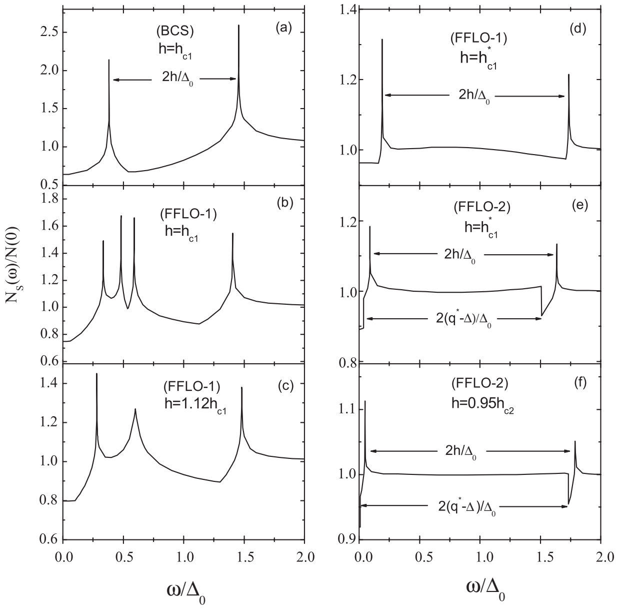

Fig. 3 – The schematic evolutionary process of $N_S(\varpi)$ at $T = 0.022T_c$. h_{c1}, h^*_{c1} and h_{c2} are the same as those given in fig. 2.

Above $T = 0.5T_c$, the superconducting state is the zero-momentum pairing BCS state with $d_{x^2-y^2}$ symmetry, which undergoes a second-order transition to the normal state at critical magnetic field h_{c2}. It is found that, in this temperature region the response of the DOS to the magnetic field can be simply characterized by the dynamics of two BCS resonant peaks. The field-dependent positions of this two peaks are $\varpi_{1,2} \approx |h \pm \Delta|$, and the separation between two peaks is $2h$ for $h < \Delta$, and 2Δ for $\Delta < h$. In particular, near the second-order phase boundaries, where $\Delta \to 0$, a $N_S(\varpi)$ with two peaks close together at about $\varpi = h$ is found.

For $T < 0.06T_c$, as we can see form fig. 1, we encounter three types of superconducting phases: the zero-momentum pairing BCS phase for $h \leq h_{c1}$; the FFLO-1 phase for $h_{c1} \leq h \leq h^*_{c1}$; the FFLO-2 phase for $h^*_{c1} \leq h < h_{c2}$, where h_{c1} and h^*_{c1} are the temperature dependent critical magnetic field corresponding to the lower and the upper first-order phase transition, respectively. Figure 2 illustrates the evolutionary process of the DOS at $T = 0.022T_c$. For $h \leq h_{c1}$, where $h < \Delta$ is always satisfied and thus the evolution may be characterized by a monotonic increase of the separation between the two peaks, as discussed above. Depicted in fig. 3(a) is the corresponding $N_S(\varpi)$ at $h = h_{c1}$. Across the lower first-order phase boundary, however, the situation is changed drastically. In the FFLO-1 phase, the evolution starts from a new structure where $N_S(\varpi)$ exhibits four peaks locating at the characteristic points $\varpi \approx |h \pm \Delta \pm q^*|$ (see fig. 3(b)). With the increase of the magnetic field, the central two peaks in $N_S(\varpi)$ merge into one peak first (see fig. 3(c)), and then this central peak gradually disappears at higher magnetic fields, leaving finally $N_S(\varpi)$ of the shape depicted in fig. 3(d). Shown in figs. 3(e) and 3(f) are, respectively, the DOS spectrum at the upper first-order phase boundary $h = h^*_{c1}$, and that at $h = 0.95h_{c2} > h_{c1}$ in the FFLO-2 phase. Comparing fig. 3(d) with fig. 3(e), one can see the new features in $N_S(\varpi)$ brought by first-order phase transition; $N_S(\varpi)$ now undergoes discontinuous changes at $\varpi = |h \pm (\Delta - q)|$. We note that, in the previous theory [6], $N_S(\varpi)$ was discussed only within the limit $T \to 0, h \to h_{c2}$.

Now we turn to consider the intermediate-temperature region $0.06T_c \leq T < 0.56T_c$, where the zero-momentum pairing BCS phase and the FFLO-1 phase are dealt with. It is confirmed up to $T = 0.4T_c$ that the evolutionary processes of $N_S(\varpi)$ in both phases are quite similar to that of the lower-temperature case and thus can also be described properly by means of figs. 3(a)-(d), with h^*_{c1} in fig. 3(d) replaced by h_{c2}. It implies that $N_S(\varpi)$ is exceptionally sensitive to the magnetic field near to the upper tricritical point. We emphasize here that, although $N_S(\varpi)$ in fig. 3(d) is of two-peak structure, the separation between the two peaks is $2h(\gg \Delta)$; it is in strong contrast to the zero-momentum pairing BCS case mentioned above.

Summary. – In summary, we have studied the response of the quasi-two-dimensional $d_{x^2-y^2}$ superconducting system to the parallel magnetic field. A complete (T, H)-phase diagram is obtained by computing the free energy. The superconducting state is separated into three phases: the zero-momentum pairing BCS phase and the two types of finite-momentum pairing phases; the FFLO-1 and the FFLO-2 phase. The phase transitions between the normal state and the superconducting states are found to be of second order, while that between the superconducting states of first order. We observe that the superconducting DOS of the FFLO phase is different significantly from that of the zero-momentum pairing BCS phase not only in its structure but also in its evolution process. In previous studies, some other important effects, *e.g.*, the weak orbital [9] and impurity scattering effects [7,10], the Fermi surface effect [11] as well as that due to the spatial structure of the order parameter [12] are not fully considered. These effects may affect the orientation of the pairing momentum $\boldsymbol{q}$, lead to changes in the location of the phase boundary and alter the nature of criticality. However, the intrinsic properties of the $d_{x^2-y^2}$ pairing FFLO state revealed by the present study seem to be robust with respect to such effects [4,12]. Our observations suggest that the FFLO state might be detected directly by means of the tunneling experiments, *e.g.* the scanning tunneling microscopy experiment.

Additional Remark. – After this letter was submitted, a related study giving the same phase diagram appeared [12].

* * *

The author is thankful to Prof. Gang Su for helpful discussions.

REFERENCES

[1] Fulde P. and Ferrell R. A., *Phys. Rev.*, **135** (1964) 550.
[2] Larkin A. I. and Ovchinnikov Yu. N., *Sov. Phys. JETP*, **20** (1965) 762.
[3] Casalbuoni R. and Nardulli G., *Rev. Mod. Phys.*, **76** (2004) 263, and references therein.
[4] Won H., Maki K., Haas S., Oeschler N., Weickert F. and Gegenwart P., *Phys. Rev. B*, **69** (2004) 180504.
[5] Maki K. and Won H., *Czech. J. Phys.*, **46** (1996) 1035.
[6] Maki K. and Won H., *Physica B*, **322** (2002) 315.
[7] Yang K. and Sondhi S. L., *Phys. Rev. B*, **57** (1998) 8566.
[8] Yang K. and Agterberg D. F., *Phys. Rev. Lett.*, **84** (1999) 4970.
[9] Klein U., Rainer D. and Shimahara H., *J. Low Temp. Phys.*, **118** (2000) 91.
[10] Agterberg D. F. and Yang K., *J. Phys. Condens. Matter*, **13** (2004) 9259.
[11] Shimahara H. and Moriwake K., *J. Phys. Soc. Jpn.*, **71** (2002) 1234.
[12] Vorontsov A. B., Sauls J. A. and Graf M. J., cond-mat/0506257 (unpublished).